Study of chemical bath deposited Cu(In,Al)Se$_2$ thin films as an alternate candidate for solar cells

B. Kavitha* and M. Dhanam

Kongunadu Arts and Science College, Coimbatore, Tamilnadu, India-641029. India.

Cu(InAl)Se$_2$ (CIAS) thin films of different thicknesses were prepared by a chemical bath deposition technique(CBD) onto well-cleaned substrates and the thicknesses of the deposited films were determined by a gravimetric technique. The films are investigated with X-ray diffraction, scanning electron microscopy and optical spectroscopy. The structural characterization was carried out by X-ray diffraction which confirms the polycrystalline nature of the films with a tetragonal structure. SEM analysis of the films enabled the conclusion that the prepared films are uniform, smooth and polycrystalline. From the transmittance spectra the type of transition and band gaps of the films were estimated. From the results of the structural and optical analysis, CIAS has been identified as an alternate solar cell absorber.

Key words: CIAS, XRD, SEM, CBD.

Introduction

Thin film solar cells based on chalcopyrite thin films have gained increasing interest due to steady progress in conversion efficiencies [1]. Solar cells based on chalcopyrite compound CuInSe$_2$ [CIS] thin films have emerged as a leading absorber candidate for low cost solar electric power generation for the last twenty years [1]. Several recent advances have been made to improve its band gap [E$_g$]. The band gap of CIS can be increased to match the solar spectrum for higher efficiency by alloying with group III or IV elements. Extensive research work has been carried out on Cu(In,Ga)Se$_2$ [CIGS] and CuIn(S,Se)$_2$ [CISS] alloy systems. Significant effort has been made to develop high-efficiency solar cells with an increased band gap by gallium additions i.e. CuIn$_{1-x}$Ga$_x$Se$_2$ films and devices. An increase in E$_g$ of the absorber layer results in a tradeoff of higher open circuit (V$_{oc}$) and lower short circuit current (J$_{sc}$) for the solar cells [2]. A further wider band gap absorber layer could be used to develop multijunction devices with even higher efficiency [3]. Thin film solar cells based a CIGS absorber showed an efficiency of ~ 19% [4]. The band gap of CIGS can be varied from 1.0 to 1.7 eV. However with band gaps greater than 1.3 eV the efficiency of CIGS devices is limited by a degradation of the electronic properties of the CIGS layer leading to losses in the fill factor (FF) and open circuit voltage (V$_{oc}$) and a decrease in the junction quality factor [5, 6]. Cu(InAl)Se$_2$[CIAS] may be a viable alternative for higher band gap CIS- based solar cells because it requires

a smaller relative alloy concentration than Ga or S alloys to achieve a comparable band gap.

Earlier workers have employed evaporation methods [2, 3, 7, 8] for depositing CIAS thin films. Of the various methods the chemical bath deposition technique, a non-vacuum electroless technique, has many advantages such as simplicity, no requirement for sophisticated instruments, minimum material wastage, economical way of depositing large areas and no need of handling poisonous gases [9]. More than that no researchers have analyzed CIAS thin films prepared by an economic chemical bath deposition (CBD) technique and therefore focus has been given to CBD CIAS thin films. In earlier work XRD and transmittance spectra have been employed to find the In and Al composition in CIAS thin films [10]. This paper enables one to identify CBD CIAS thin films as an alternate solar cell absorber material from its structural and optical analysis.

Experimental Procedure

The deposition of CIAS thin films is based on the reaction of Cu^{2+} with In^{3+}, Al^{3+} and Se^{2-} ions in a deionized water solution. Chemical baths used for the deposition of CIAS thin films consist of copper sulphate, trisodium citrate, indium trichloride, selenous acid, aluminum sulphate and citric acid. Chemical baths containing the same reaction mixture of 7.5 ml (0.2 M) CuSO$_4$ solution, 7.5 ml (0.1 M) trisodium citrate solution, 6.25 ml (0.1 M) InCl$_3$ solution (CDH), 25 ml (0.05 M) citric acid solution, 10 ml selenium solution and 6.25 ml Al$_2$SO$_4$ solution have been selected. The complexing citrate agent is used to avoid the binary formation. Trisodium citrate was used to complex copper ions in order to ensure a slow release of Cu^{2+} ions in the deposition mixture. The pH of the solution can be adjusted by adding sodium hydroxide solution.

*Corresponding author:
 Tel : +91 9486412805
 Fax: +0422-2644452
 E-mail: kavitha.sudharsan@gmail.com

A digital pH meter (model 101E-Electronic India) has been used to adjust the pH of the reaction mixture. The pH meter was standardized using buffer solutions of pH 4 ± 0.05 and 9.2 ± 0.05. The substrates used for the deposition of films were suspended closer to the inner wall of the deposition beaker for better uniformity and adherence of the film on the substrate and to avoid shaking of substrates during the deposition [11]. The depositions were carried out in water baths at different temperatures from 40 to 60 °C. A constant and very slow stirring was provided while adding the different solutions of the reacting mixture. The deposition time was varied from 30 minutes to 180 minutes to obtain films of different thicknesses. Uniform films were obtained for a deposition time between 30 minutes to 90 minutes. While varying the pH of the bath, it was found that the solution having a pH value 10 (chemical bath 1) and 9 (chemical bath 2) gave uniform films. Thus deposition parameters such as temperature, concentration of ions in the bath and dipping time have been optimized and then the films were taken out and dried naturally. Three representative films (1-3) were employed for the study. Films 1&2 differ only in pH (i.e.) they have pH values of 10 and 9 respectively. Film 3 has the same pH as that of bath 1 but the pH adjustments have been varied after heating the solution to 50 °C for 10 minutes whereas films 1 and 2 have been prepared from the chemical baths in which pH of the reaction mixture is adjusted to 10 and then heated to 50 °C for 10 minutes.

A Shimadzu XRD-6000 X-ray diffractometer with a vertical goniometer fitted with vanadium filter and copper radiation ($\lambda = 1.5406$ Å) with a step size of 1.01° was used for the structural analysis of the films of different thicknesses. The surface morphology of CIAS thin films was studied using a scanning electron microscope (JEOL JSM 6330 F). A JASCO (V570:UV-VIS-NIR) double beam spectrophotometer was used for optical studies in the wavelength range 400-2500 nm.

Results

Structural analysis of CIAS thin films from XRD profiles

X-ray diffraction patterns of the CIAS thin films deposited are presented in Fig. 1 which confirms the polycrystalline nature of prepared CIAS films. From the diffraction profiles the diffraction angles and the intensity of lines may be measured with greater accuracy. The absence of broadening of the peaks suggest that the CIAS films prepared are free from stress and that may be the reason for better adhesion [10].

The predicted peaks (112) (211) (301) (220/204) and (105) are reported as the identifying peaks for CIAS thin films in earlier studies [3, 5, 7, 8] and JCPDS file [40-1487]. As reported by Halgand *et al*. [7] due to the non-availability of a JCPDS file for CIAS, the CIS standard has been used in the present study. The presence of these prominent peaks confirm the chalcopyrite structure of the
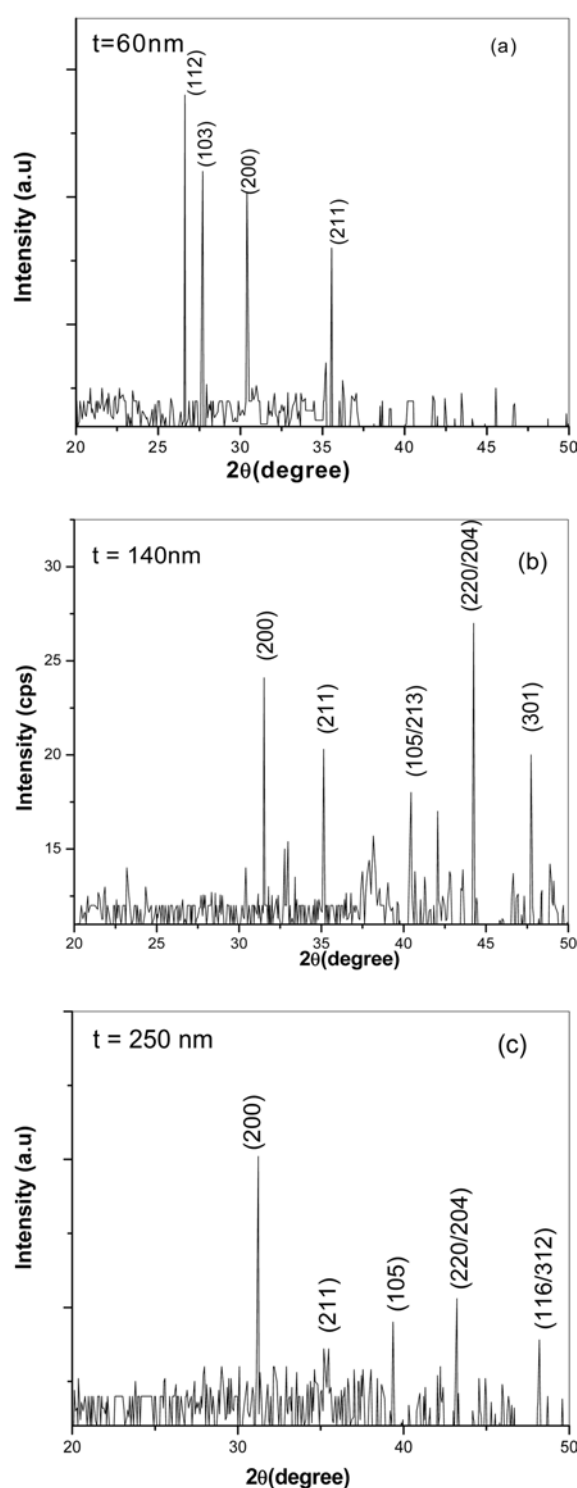
Fig. 1. (a) X-ray diffractogram of CIAS film 1, (b X-ray diffractogram of CIAS film 2, (c) X-ray diffractogram of CIAS film 3.

as-grown CIAS films. From the diffraction profiles it has been found that the films are polycrystalline in nature with a tetragonal structure having a preferred orientation along (112) or (220/204) or (101) planes. The peaks corresponding to the (200) plane were due to reflection from the substrate [12]. The enhancement of the planes and in turn the improved crystanality with film thickness is remarkable

Table 1 Structural parameters of CBD CIAS thin films of different thicknesses

Film Thickness (nm)	Lattice Constants (Å)				axial ratio c/a	tetragonal distortion (2-c/a)	Volume of the unit cell (Å)³		Crystallite size Dᶜ (nm)	Dislocation density (10¹⁵ lines/m²)	Number of crystallites per unit area (10¹⁵ m⁻²)	Strain × 10⁻³
	a		C									
	Observed	ASTM	Observed	ASTM			Observed	ASTM				
1 60	5.785		11.616		2.06	-0.06	388.8		29	1.189	2.460	1.273
2 140	5.783	5.782	11.018	11.619	1.90	0.094	386.2	388.4	60	0.277	0.648	0.606
3 250	5.784		10.779		1.86	0.13	385.4		91	0.120	0.331	0.404

irrespective of the chemical bath [13].

From the observed 'd' spacing and (hkl) planes the lattice constants were evaluated using the relation [14, 15]:

$$d^2 = \frac{a^2}{h^2 + l^2} + \frac{c^2}{l^2} \qquad (1)$$

where 'd' is the d-spacing and 'a and c' are the lattice parameters. The lattice parameters are in agreement with the JCPDS data [40-1487] and earlier reports [2, 3, 5, 7, 8, 16]. From the observed d-spacing various structural parameters such as the lattice constants ('a' and 'c'), the axial ratio, the tetragonal distortion, the volume of the unit cell, the crystallite size, the dislocation density and number of crystallites per unit area and strain have been estimated using standard expressions [9] are presented in Table 1. The defects such as dislocation density and strain decreases with increasing film thicknesses which is due to the improvement in crystallnity in the films. The thickness dependence of grain size, strain and dislocation density is similar in all the three the films but they differ only in their preferential orientation. The structure, prominent peaks and structural parameters of CIAS are very similar to CIS thin films [9, 12, 17].

Surface morphological studies

Fig. 2(a) reveals that the deposited film (Film 1) has a distribution with a reasonably low defect density and a good crystalline quality and the film surface has a generally smooth and dense morphology [18, 19]. Fig. 2(b) shows a uniform and smooth morphology of the grown film (Film 2) containing an accumulation of small grains and here the deposit distribution is less porous and this CIAS film is polycrystalline in nature. Fig. 2(c) image has cracks all over the film (Film 3) and this may be due to the contamination in the films caused by adjustments in the pH after heating the reaction mixture and which may be eliminated by etching [20, 21].

Optical properties

The absorbance of the films increases with film thickness (Fig. 3) and similarly the transmittance of the films (not shown) prepared from the chemical baths decreases as the film thickness increases. From a quantum mechanical basis and appropriate selection rules, it is possible to find out the nature of the electronic transition from the absorption of photon energy by using the relation:

(a)

(b)

(c)
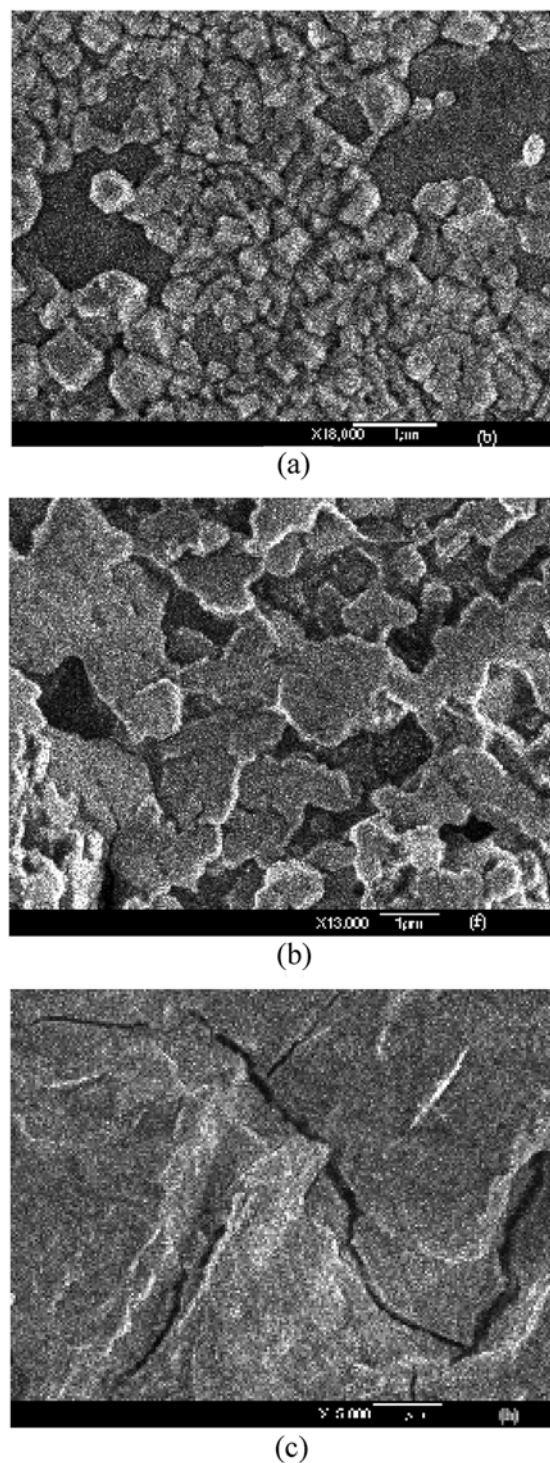
Fig. 2. (a) SEM image of CIAS film 1, (b) SEM image of CIAS film 2, (c) SEM image of CIAS film 3.
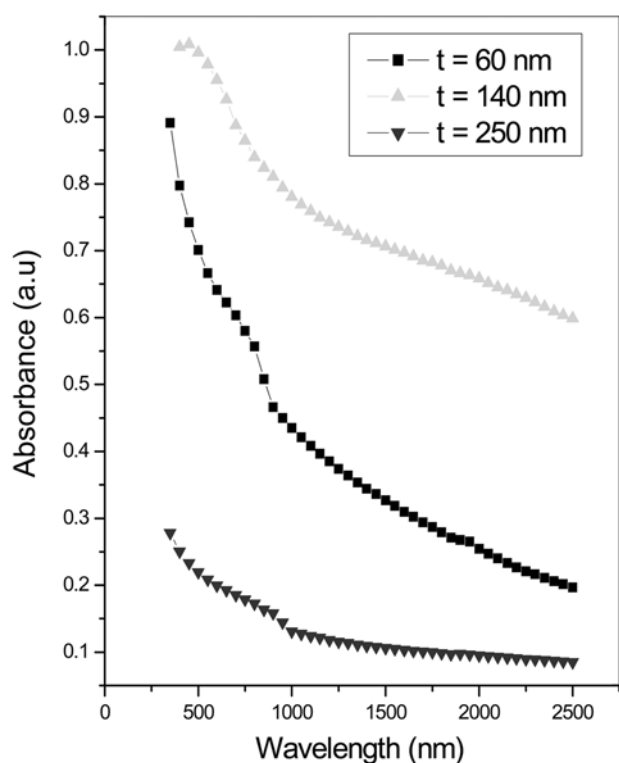
Fig. 3. Absorbance spectra of CBD CIAS thin films of different thicknesses.

Table 2 Summarized results of optical properties of chemical bath deposited CIAS thin films

Film	Thickness	Absorption coefficient $(\alpha) \times 10^6 \, \text{m}^{-1}$	Extinction coefficient (k)	Band gap Eg (eV)
1	60	17.170	1.367	1.35
2	140	1.244	0.099	1.30
3	250	0.122	0.009	1.24

$$\alpha = \frac{A(hv - Eg)^r}{hv} \qquad (2)$$

where A is a constant and E_g is the energy band gap. The optical energy band gap is the minimum energy required to excite an electron from the valance band to the conduction band by an allowed optical transition [22]. The summarized results of optical properties of CIAS thin films are presented in Table 2. A plot of $(\alpha\upsilon)^2$ versus $(h\upsilon)$ for CIAS thin films of different thicknesses is shown in Fig. 4. The straight line extrapolated to the energy axis has been rotated many times and the band gap has been estimated each time and the average values of Eg are given in Table 3. Direct allowed band gaps of 1.24 eV to 1.35 eV has been obtained for CIAS films of different thicknesses, which reveal the presence of direct allowed transitions in CIAS thin films. The observed band gap values are in agreement with earlier reported values [2, 3, 5, 7, 8] and from the optical study it has been confirmed that the band gap of CIAS (1.24-1.35 eV) is higher than the reported band gap of CIS (1 eV) [9, 12, 23].
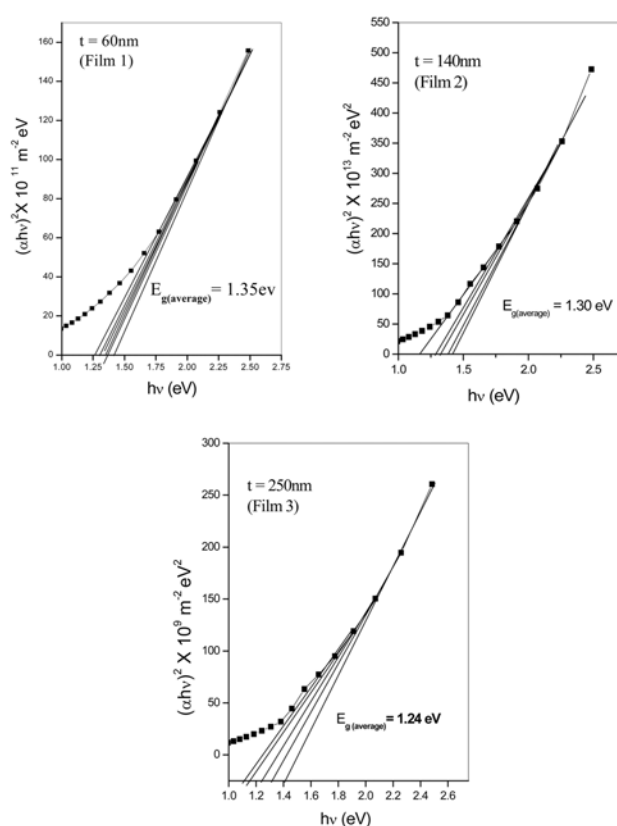
Fig. 4. Plot of $(\alpha\upsilon)^2$ vs. $(h\upsilon)$ of CIAS thin films of three different films.

Table 3 Determination of $E_{g(average)}$ of CIAS thin films

Films	S.No of rotations	Band gap (eV)	$E_{g \, (average)}$ (eV)
Film 1	1.	1.19	1.35
	2.	1.27	
	3.	1.30	
	4.	1.35	
	5.	1.40	
Film 2	1.	1.18	1.30
	2.	1.24	
	3.	1.31	
	4.	1.33	
	5.	1.41	
Film 3	1.	1.10	1.24
	2.	1.14	
	3.	1.24	
	4.	1.31	
	5.	1.42	

Conclusions

X-ray diffraction and scanning electron microscope studies of CBD CIAS thin films confirmed that the films prepared are polycrystalline in nature with a tetragonal structure. The structural parameters are very much comparable with the leading absorber candidate CIS. SEM analysis of the films enabled one to conclude that the prepared films are uniform, smooth and polycrystalline. From the optical analysis it is concluded that the band gap of the films have been widened compared to CIS. Thus from

structural and optical study, CIAS has been identified as a suitable alternate absorber candidate for solar cells.

Acknowledgements

References

1. BÜlent M. Başol, Vijay K. Kapur, Arvind Halani and Craig Leidholm, Solar Energy Materials and Solar Cells, 29 (1993) 163-173.
2. P.D. Paulson, M.W. Haimbodi, S. Marsillac, R.W. Birkmire and W.N. Shafarman, Journal of Applied Physics, 91 (2002) 10153-10156.
3. S. Marsillac, P.D. Paulson, M.W. Haimbodi and W.N. Shafarman, Applied Physics Letters, 81[7] (2002) 1350-1352.
4. M.A. Contreras, B. Egaas, K. Ramanathan, J. Hiltner, A. Swartzlander, F. Hasoon and R. Noufi, Prog. Photovoltaics. Res.Applied, 7 (1999) 311-315.
5. W.N. Shafarman, R. Klenk and B.E. McCandless, Journal of Applied Physics, 79 (1996) 7324-7328.
6. U. Rau, M. Schmidt, A. Jasenek, G. Hanna and H.W. Schock, Solar Energy Materials and Solar Cells, 67 (2001) 137-143.
7. E. Halgand, J.C. Bernede, S. Marsillac and J. Kessler, Thin Solids Films, 480-481 (2005) 443-446.
8. E. Itoch, O. Saitoh, M. Kita, H. Nagamori and H. Oike, Solar Energy Materials and Solar Cells, 50 (1998) 119-125.
9. M. Dhanam, R. Balasundarprabhu, S. Jayakumar, P. Gopalakrishnan and M.D. Kannan, Physica Status Solidi (a), 19[1] (2002) 149-160.
10. B. Kavitha and M. Dhanam, Journal of Material Science and Engineering: B, 140 (2007) 59-63.
11. M. Dhanam, P.K. Manoj, Rajeev and R. Prabhu, Journal of Crystal Growth 280 (2005) 425-435.
12. M. Dhanam, S. Jayakumar and M.D.Kannan, Bulletin of Electrochemistry, 14[11] (1998) 418-421.
13. F.J. Pern, R. Noufi, A. Manson and A. Franz, Thin Solid Films, 202 (1999) 299-314.
14. S.L. Gupta and V. Kumar, Solid State Physics, K.Nath & Co., Seventh Edition, Meerut, (1988-89).
15. A. Goswami, Thin Film Fundamentals, New Age International (P) Limited Publishers, New Delhi, (1996)
16. Y. Bharath Kumar Reddy and V. Sundara Raja, Solar Energy Materials and Solar Cells, 90 (2006) 1656-1665.
17. J.c. Garg, R.P. Sharma and K.C. Sharma, Thin Solid Films, 164 (1988) 269-273.
18. M.S. Sadigov, M. Özkan, E. Bacaksiz, M.A. Hunbas and A.I. Kopya, Journal of Materials Science, 34 (1999) 4579-4584.
19. J.W. Park, G.Y. Chung, B.T. Ahn and H.B. Im and J.S. Song, Thin Solid Films, 245 (1994) 174-179.
20. C.D. Lokande, Journal of Electrochemical Society, 134 (1987) 1727-1729.
21. J.C.Bernède and L.Assmann, Vacuum, 59 (2000) 885-893.
22. Y. Bharath Kumar Reddy and V. Sundara Raja, Semiconductor Science and Technology, 19 (2004) 1015-1019.
23. R.P. Sharma, K.C. Sharma and J.C. Garg, Journal of Physics D: Applied Physics, 24 (1991) 2084-2087.